Science Advances
AAAS

Supplementary Materials for

Environmental eustress improves postinfarction cardiac repair via enhancing cardiac macrophage survival

Pei-Yuan Bai, Si-Qin Chen, Dai-Le Jia, Li-Hong Pan, Chao-Bao Liu, Jin Liu, Wei Luo, Yang Yang, Ma-Yu Sun, Nai-Fu Wan, Wu-Wei Rong, Ai-Jun Sun*, Jun-Bo Ge

*Corresponding author. Email: sun.aijun@zs-hospital.sh.cn

Published 27 April 2022, *Sci. Adv.* **8**, eabm3436 (2022)
DOI: 10.1126/sciadv.abm3436

The PDF file includes:

Figs. S1 to S16
Tables S1 and S2
Legends for movies S1 and S2

Other Supplementary Material for this manuscript includes the following:

Movies S1 and S2

Fig. S1

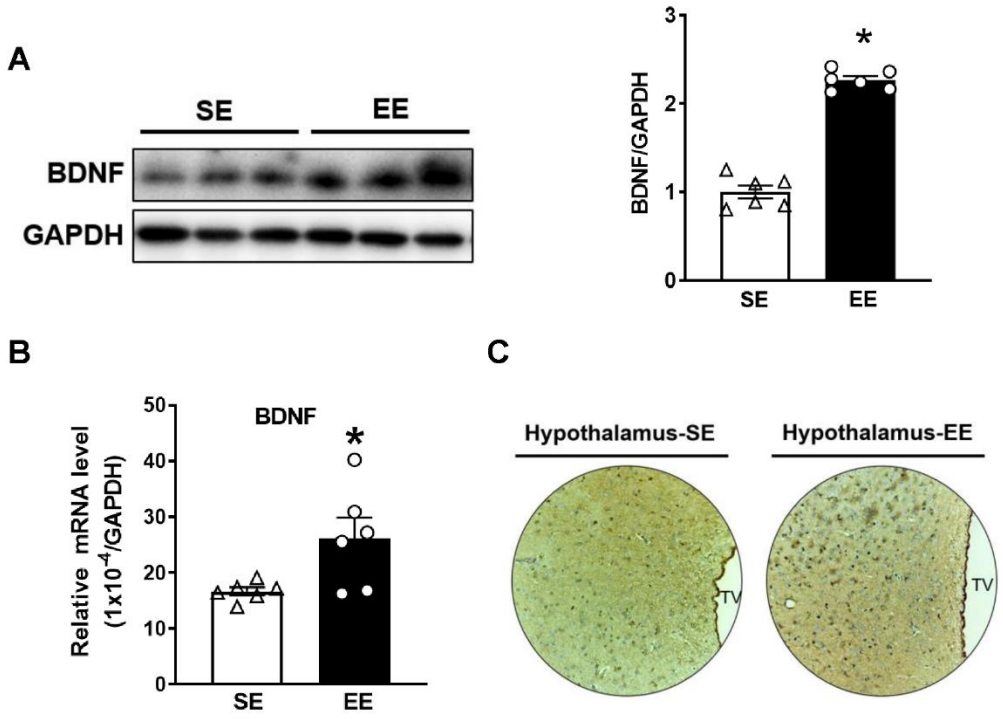

Fig. S1. Verification of successful establishment of the EE model. (A) Western blotting analysis of BDNF expression level in the hypothalamus of mice after 4 weeks of SE or EE treatment (n=6). *P <0.05 vs. SE. **(B)** *BDNF* mRNA expression levels in the hypothalamus of mice with 4 weeks of SE and EE treatment (n=6). *P <0.05 vs. SE. **(C)** Representative immunohistochemistry showed the expression of BDNF in the hypothalamus of mice with 4 weeks of SE and EE treatment. TV, third ventricle. Data are expressed as mean ± SEM. Data were analyzed using Student's t-test.

Fig. S2

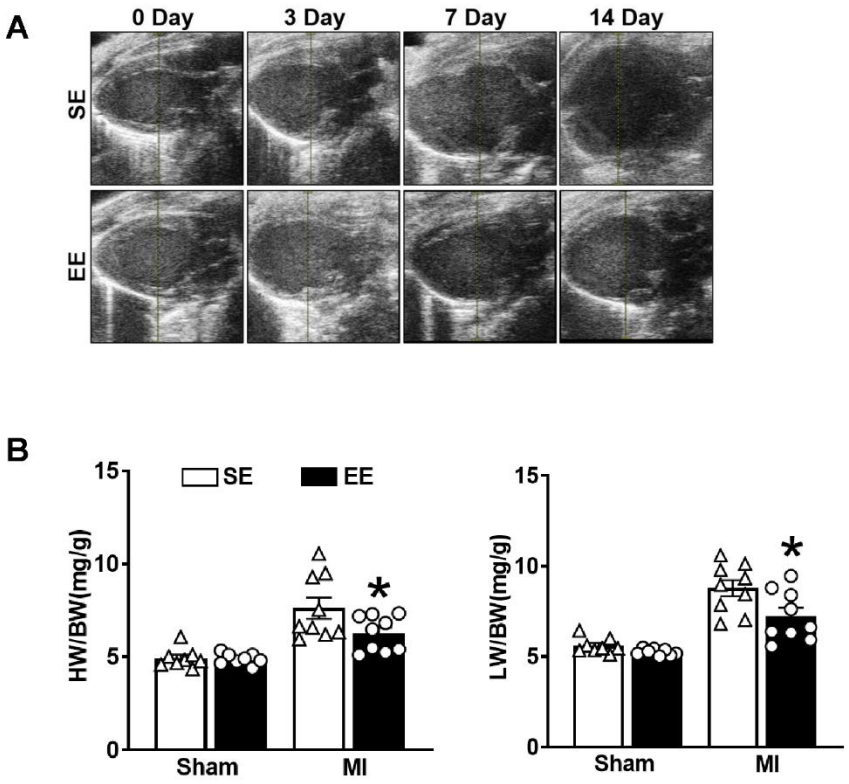

Fig. S2. EE attenuates heart failure after MI. (A) Typical B-mode images of the hearts obtained from mice at days 3, 7, and 14 after MI or sham surgery. **(B)** Comparison of the HW/BW (mg/g) and LW/BW (mg/g) values in SE and EE-induced mice after MI or sham surgery. HW, heart weight, LW, lung weight, BW, body weight (n =8-9). *P <0.05 vs. SE. Data are expressed as mean ± SEM. Data were analyzed using Student's t-test.

Fig. S3

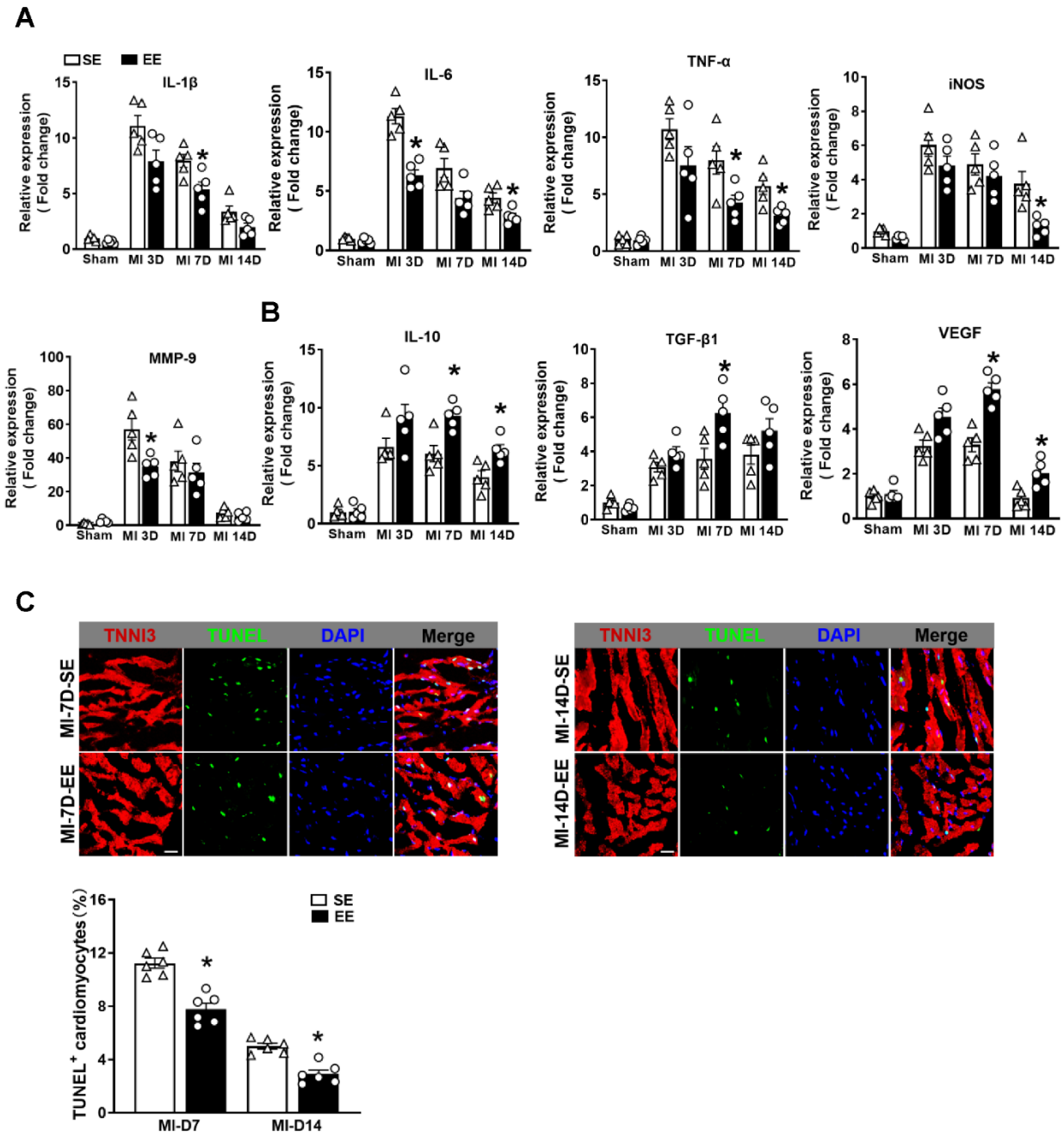
A
SE
EE
IL-1β
IL-6
TNF-α
iNOS
Relative expression (Fold change)
Sham
MI 3D
MI 7D
MI 14D
B
MMP-9
IL-10
TGF-β1
VEGF
C
TNNI3
TUNEL
DAPI
Merge
MI-7D-SE
MI-7D-EE
MI-14D-SE
MI-14D-EE
TUNEL+ cardiomyocytes (%)
MI-D7
MI-D14

Fig. S3. Effects of EE on inflammatory cytokine levels and cardiomyocyte apoptosis. (A) Major pro-inflammatory gene mRNA expression levels (IL-1β, IL-6, TNF-α, iNOS, and MMP-9) in the MI tissues obtained from the SE and EE mice at different time points after MI or sham surgery (n=5). **P*<0.05 vs. SE. **(B)** Major anti-inflammatory gene mRNA expression levels (IL-10, TGF-β1, and VEGF) in the MI tissues obtained from the SE and EE mice at different time points after MI or sham surgery (n=5). **P*<0.05 vs. SE. **(C)** The cardiomyocyte apoptosis rate was measured in heart tissue sections at 7 and 14 days after MI by staining with TNNI3 (red), TUNEL (green), and the nuclei were stained with DAPI (blue). Scale bars, 20 μm. The percentage of $TUNEL^+$ cardiomyocytes was expressed as $TNNI3^+$ $TUNEL^+$ cells/ $TNNI3^+$ cells (n=6). **P*<0.05 vs. SE. Data are expressed as the mean ± SEM. Data were analyzed using Student's t-test.

Fig. S4

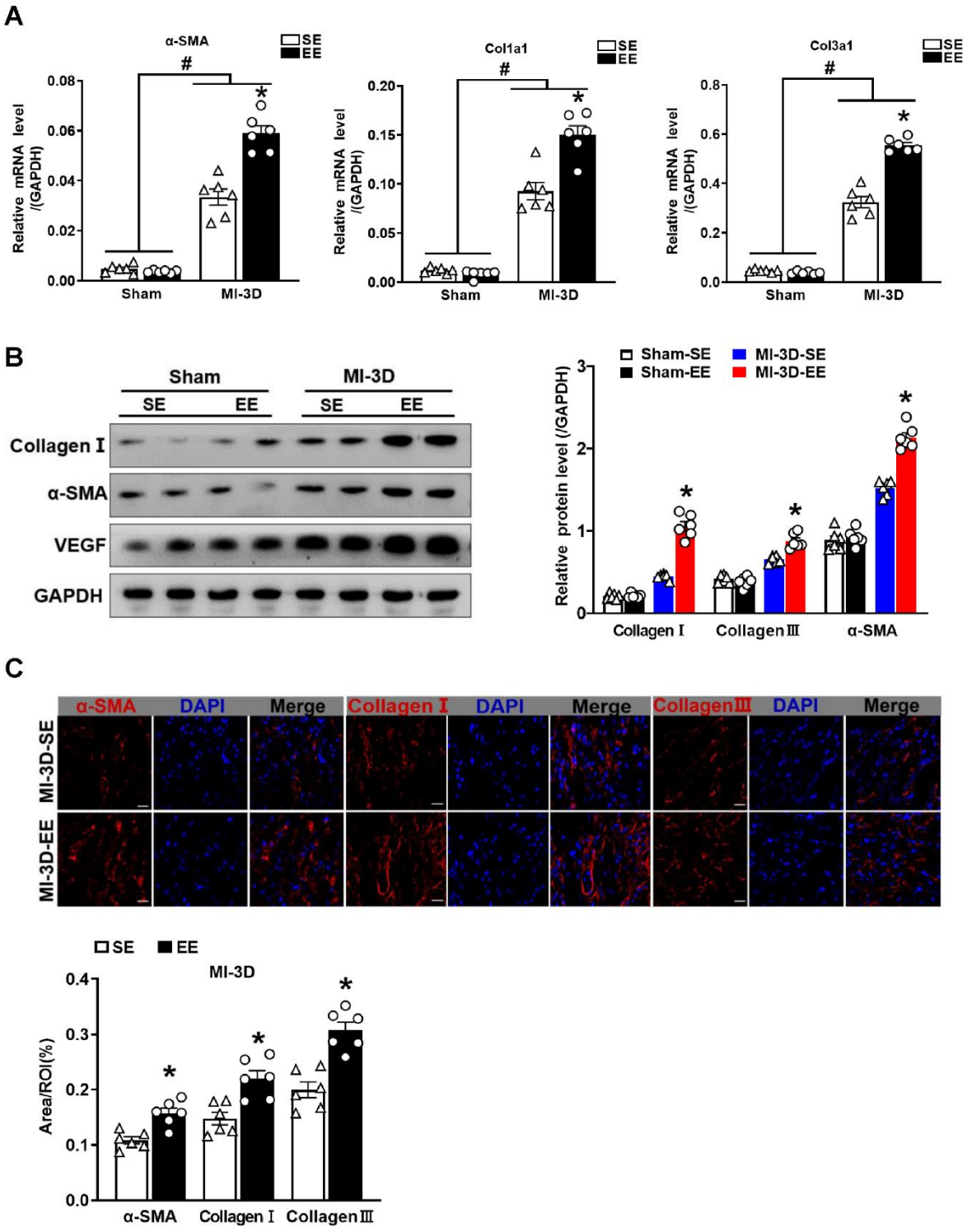
A
α-SMA
Col1a1
Col3a1
SE
EE
Relative mRNA level /(GAPDH)
Sham
MI-3D
B
Sham
MI-3D
SE
EE
Collagen Ⅰ
α-SMA
VEGF
GAPDH
Sham-SE
Sham-EE
MI-3D-SE
MI-3D-EE
Relative protein level /(GAPDH)
Collagen Ⅰ
Collagen Ⅲ
α-SMA
C
α-SMA
DAPI
Merge
Collagen Ⅰ
Collagen Ⅲ
MI-3D-SE
MI-3D-EE
MI-3D
Area/ROI(%)

Fig. S4. Effects of EE on extracellular matrix in infarcted area 3 days after MI. (A) mRNA expression of α-SMA, Collagen (Col)1a1, and Col3a1 in the scar tissues of SE and EE mice at day 3 after MI or sham surgery (n = 6). *P < 0.05 vs. SE MI. **(B)** Western blotting analyses of collagen I, collagen III, and α-SMA protein expression in the scar tissue of SE and EE-treated mice at day 3 after MI or sham surgery (n=6). *P <0.05 vs. SE. **(C)** Immunofluorescence staining analyses of α-SMA, collagen I, and collagen III in infarcts collected at day 3 after MI (Scale bars, 20 μm) (n=6). *P <0.05 vs. SE. Data are expressed as mean ± SEM. Data in **(A)** were analyzed using two-way ANOVA followed by Bonferroni post hoc analysis. Data in **(B)** and **(C)** were analyzed using Student's t-test.

Fig. S5

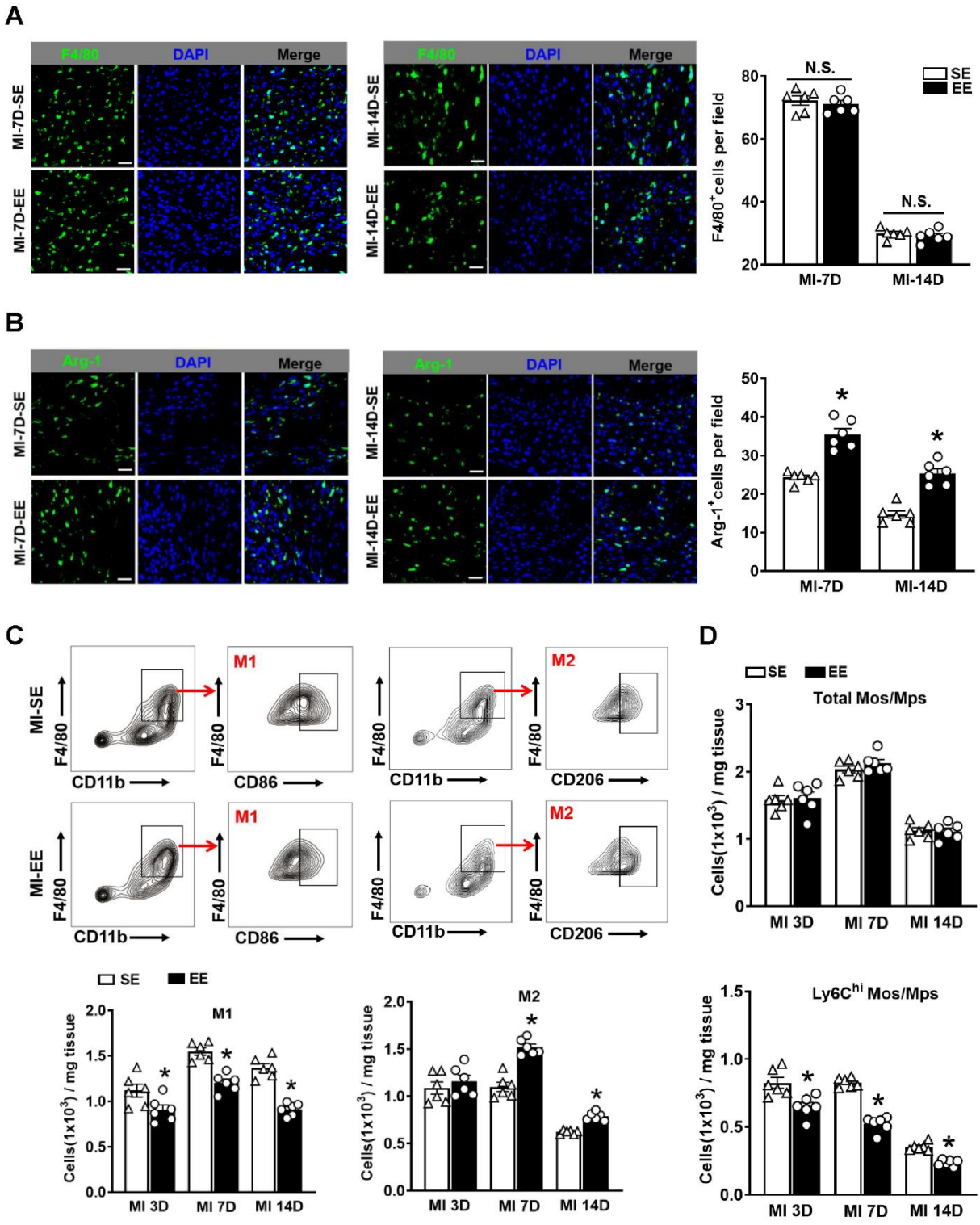
A
F4/80
DAPI
Merge
MI-7D-SE
MI-7D-EE
MI-14D-SE
MI-14D-EE
F4/80+cells per field
N.S.
SE
EE
MI-7D
MI-14D
B
Arg-1
Arg-1+cells per field
C
MI-SE
MI-EE
CD11b
CD86
CD206
M1
M2
D
Total Mos/Mps
Cells(1x10³) / mg tissue
MI 3D
MI 7D
MI 14D
Ly6Chi Mos/Mps

Fig. S5. Effect of EE on M1/M2 -like macrophages in infarct zone. (A) Immunostaining analyses of F4/80^{+} macrophages in infarct zone at days 7 and 14 post-MI (Scale bars, 20 μm). (n=6). **(B)** Immunostaining analyses of Arg-1^{+} macrophages in infarct zone at days 7 and 14 post-MI (Scale bars, 20 μm). (n=6). **(C)** Gating strategy for CD45^{+} CD11b^{+} F4/80^{+} CD86^{+} M1-like and CD45^{+} CD11b^{+} F4/80^{+} CD206^{+} M2-like macrophages in infarcts obtained from mice by 4 weeks of SE or EE treatment. Flow cytometry-based quantification of M1 and M2-like macrophages at days 3, 7, and 14 after MI (n=5-6). (**D**) Flow cytometry-based quantification of total and Ly6C^{high} Mos/Mps at days 3, 7, and 14 post-MI (n = 5–6). *P < 0.05 vs. SE. Data are expressed as mean ± SEM. Data were analyzed using Student's t-test.

Fig. S6

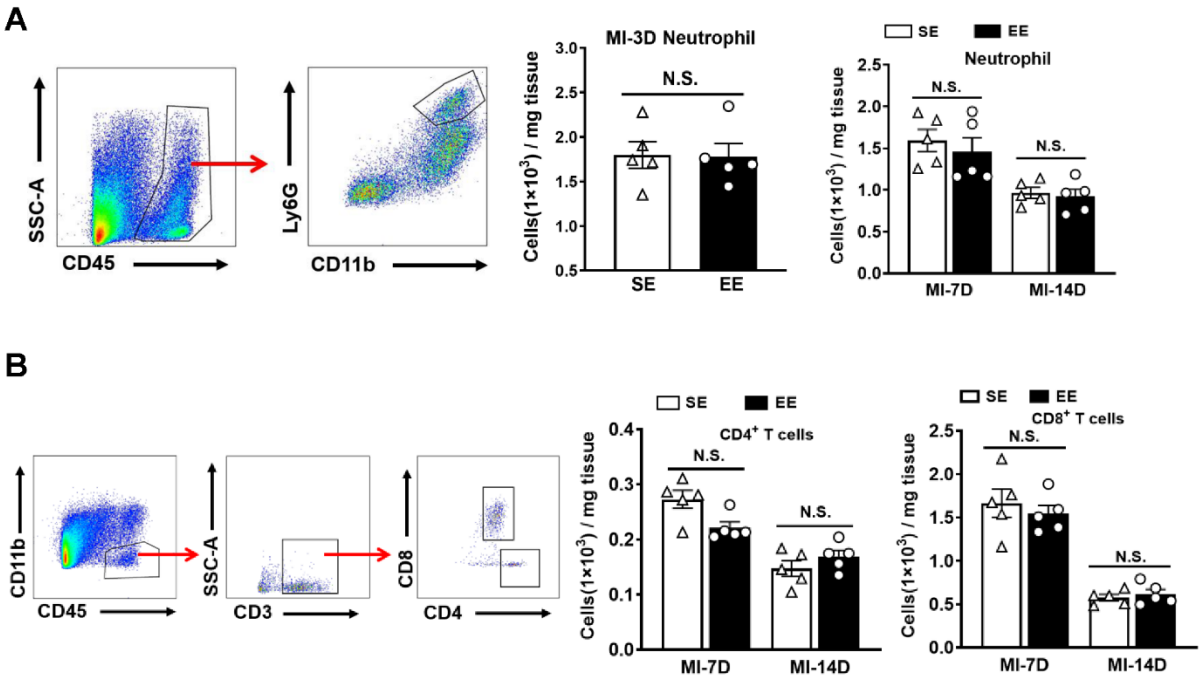

Fig. S6. Effect of EE on immune cells in infarct zone of mice. (A) Gating strategy for $CD45^+CD11b^+Ly6G^+$ neutrophils in infarcted tissues obtained from mice with 4 weeks of SE or EE treatment. Flow cytometry-based quantification of neutrophils per milligram of tissue at days 3, 7, and 14 post-MI (n=5). **(B)** Gating strategy for $CD45^+CD11b^+CD3^+CD4^+CD8^-$ and $CD45^+CD11b^+CD3^+CD4^-CD8^+$ T cells in infarcted tissues obtained from mice with 4 weeks of SE or EE treatment. Flow cytometry-based quantification of $CD4^+$ and $CD8^+$ T cells per milligram of tissue at days 7 and 14 post-MI (n=5).

Fig. S7

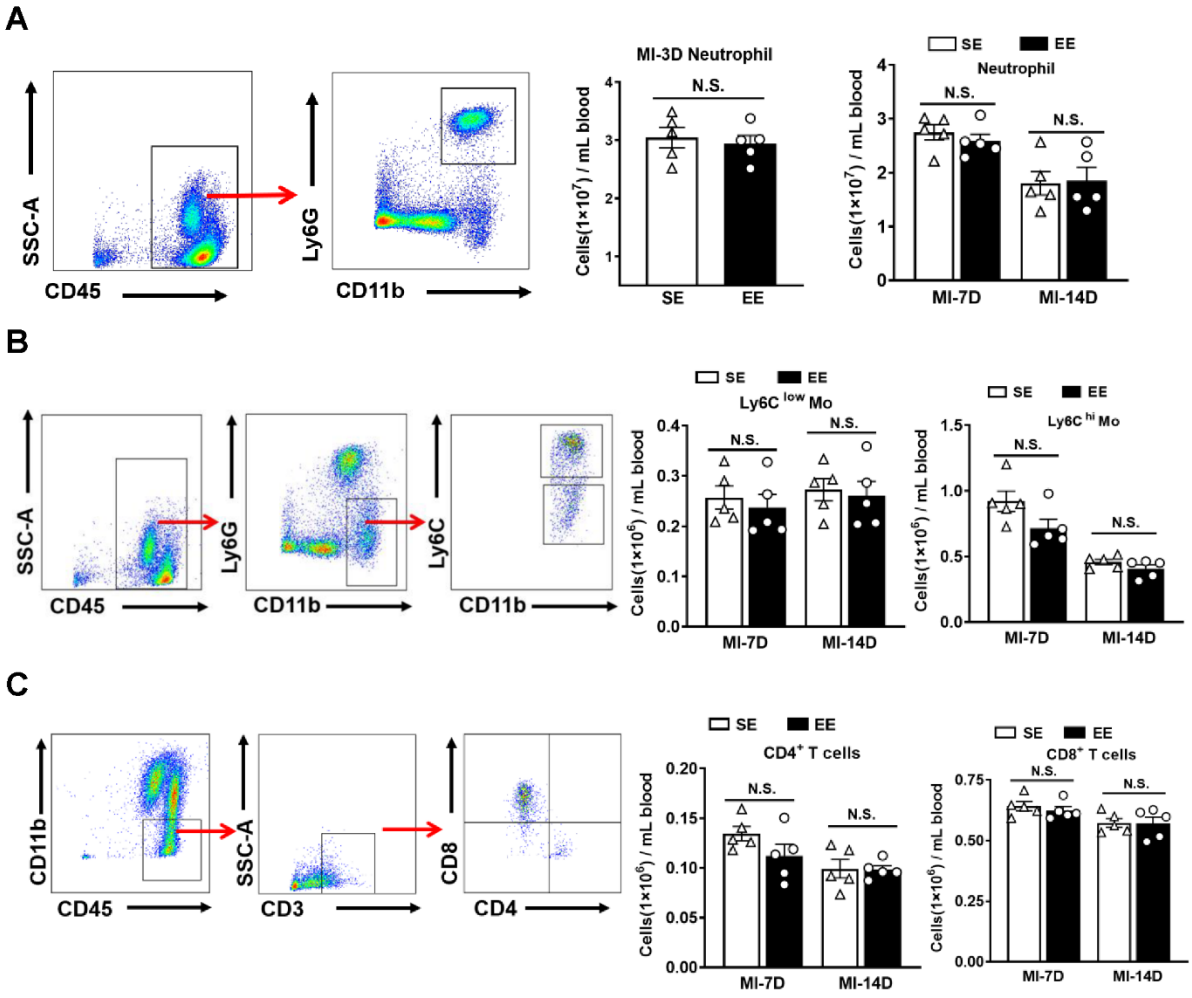

Fig. S7. Effect of EE on immune cells in peripheral blood of mice. (A) Gating strategy for $CD45^+CD11b^+Ly6G^+$ neutrophils in the peripheral blood of mice after 4 weeks of SE or EE housing. Flow cytometry-based quantification of neutrophils per milliliter of peripheral blood at 3, 7, and 14 days after MI surgery (n=5). **(B)** Gating strategy for $CD45^+CD11b^+Ly6G^-Ly6C^{low}$ and $CD45^+CD11b^+Ly6G^-Ly6C^{hi}$ monocytes in the peripheral blood of mice after 4 weeks of SE or EE housing. Flow cytometry-based quantification of $Ly6C^{low}$ and $Ly6C^{hi}$ monocytes per milliliter of peripheral blood at 7 and 14 days after MI surgery (n=5). **(C)** Gating strategy for $CD45^+CD11b^+CD3^+CD4^+CD8^-$ and $CD45^+CD11b^+CD3^+CD4^-CD8^+$ T cells in the peripheral blood of mice after 4 weeks of SE or EE housing. Flow cytometry-based quantification of $CD4^+$ and $CD8^+$ T cells per milliliter of peripheral blood at 7 and 14 days after MI surgery (n=5)

Fig. S8

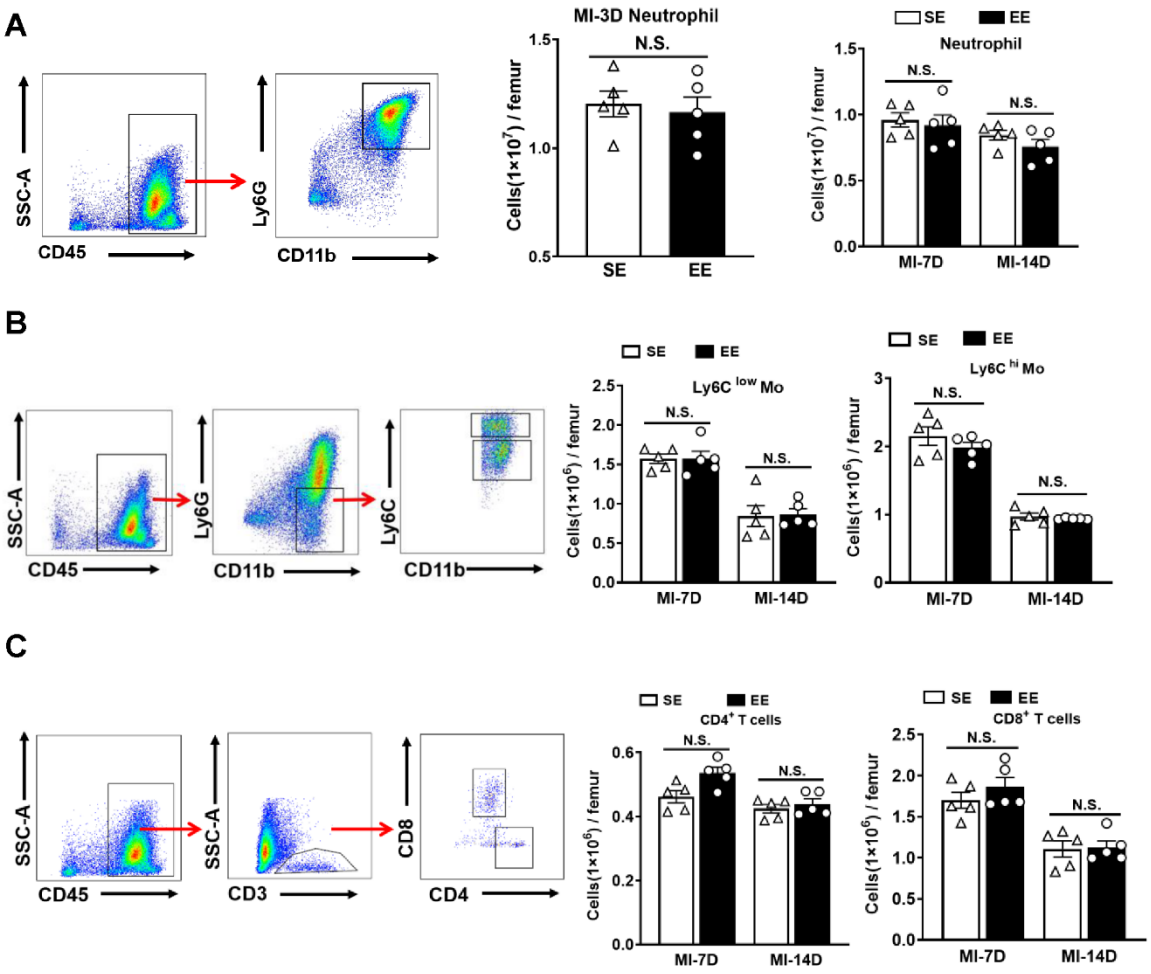

Fig. S8. Effect of EE on immune cells in the bone marrow of mice. (A) Gating strategy for $CD45^+CD11b^+Ly6G^+$ neutrophils in the bone marrow of mice after 4 weeks of SE or EE housing. Flow cytometry-based quantification of neutrophils in each femur at 3, 7, and 14 days after MI surgery (n=5). **(B)** Gating strategy for $CD45^+CD11b^+Ly6G^-Ly6C^{low}$ and $CD45^+CD11b^+Ly6G^-Ly6C^{hi}$ monocytes in the bone marrow of mice after 4 weeks of SE or EE housing. Flow cytometry-based quantification of $Ly6C^{low}$ and $Ly6C^{hi}$ monocytes in each femur at 7 and 14 days after MI surgery (n=5). **(C)** Gating strategy for $CD45^+CD11b^+CD3^+CD4^+CD8^-$ and $CD45^+CD11b^+CD3^+CD4^-CD8^+$ T cells in the bone marrow of mice after 4 weeks of SE or EE housing. Flow cytometry-based quantification of $CD4^+$ and $CD8^+$ T cells in each femur at 7 and 14 days after MI surgery (n=5).

Fig. S9

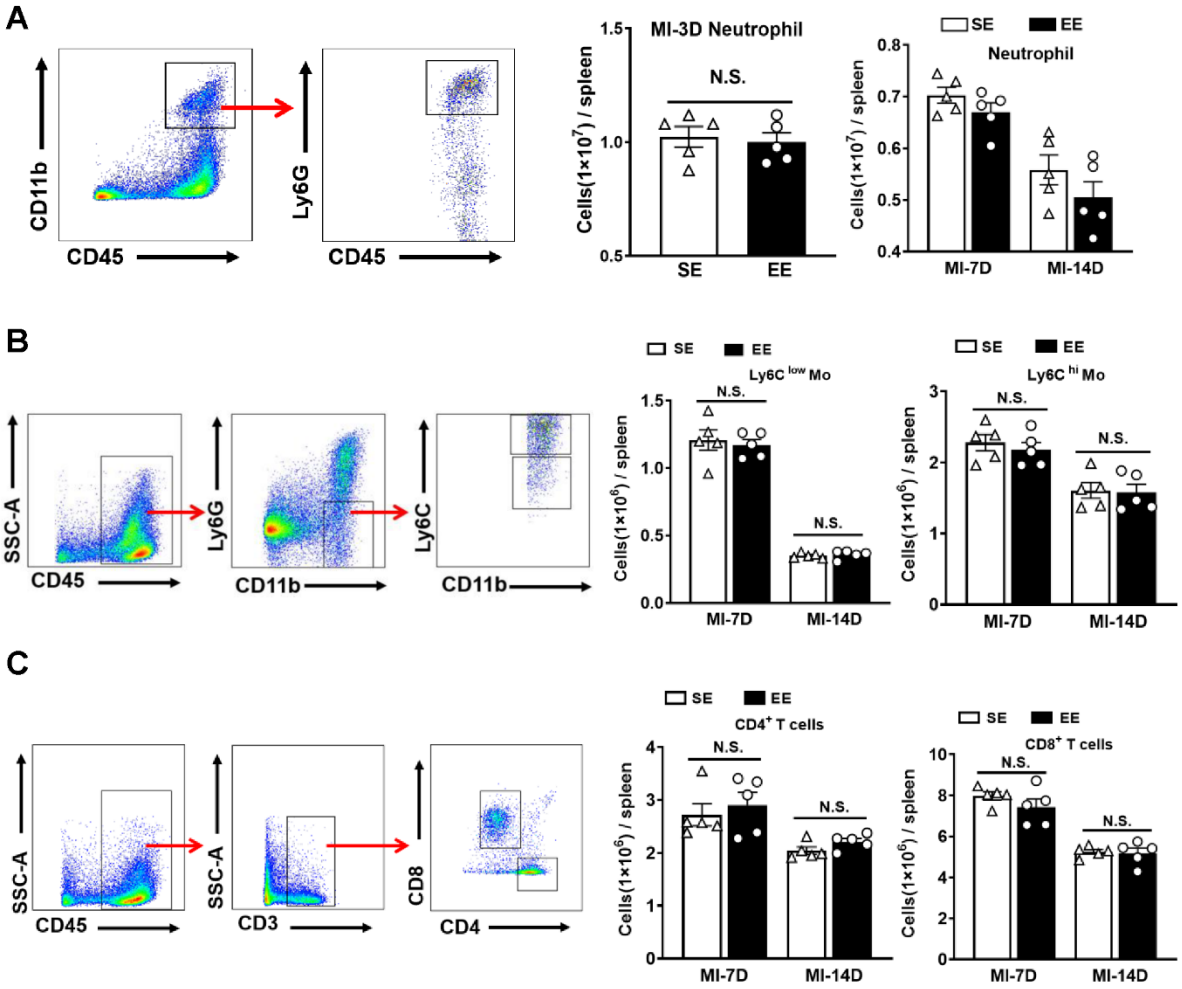

Fig. S9. Effect of EE on immune cells in the spleen of mice. (A) Gating strategy for $CD45^+CD11b^+Ly6G^+$ neutrophils in the spleen of mice after 4 weeks of SE or EE housing. Flow cytometry-based quantification of neutrophils in the spleen at 3, 7, and 14 days after MI surgery (n=5). **(B)** Gating strategy for $CD45^+CD11b^+Ly6G^-Ly6C^{low}$ and $CD45^+CD11b^+Ly6G^-Ly6C^{hi}$ monocytes in the spleen of mice after 4 weeks of SE or EE housing. Flow cytometry-based quantification of $Ly6C^{low}$ and $Ly6C^{hi}$ monocytes in the spleen at 7 and 14 days after MI surgery (n=5). **(C)** Gating strategy for $CD45^+CD11b^+CD3^+CD4^+CD8^-$ and $CD45^+CD11b^+CD3^+CD4^-CD8^+$ T cells in the spleen of mice after 4 weeks of SE or EE housing. Flow cytometry-based quantification of $CD4^+$ and $CD8^+$ T cells in the spleen at 7 and 14 days after MI surgery (n=5).

Fig. S10

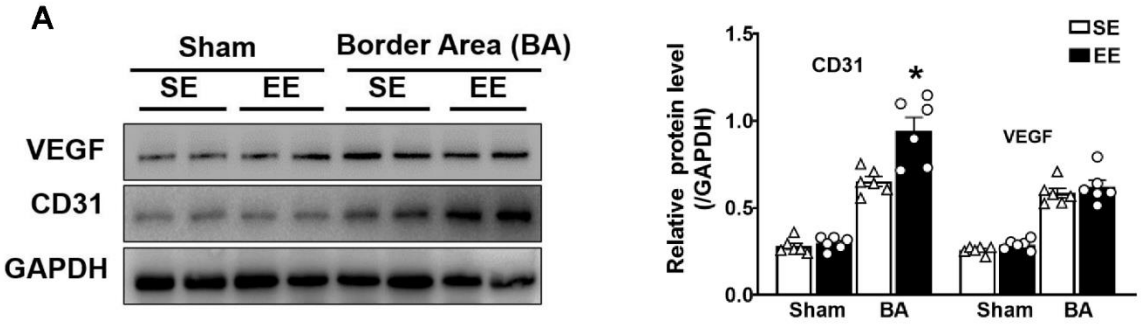

Fig. S10. Effects of EE on neovascularization in the border area at 14 days after MI. (A) Western blot analysis of VEGF and CD31 protein expression levels in the border area of the SE and EE mice at 14 days after MI or sham surgery. VEGF and CD31 protein levels were quantified by densitometry and normalized to GAPDH (n=6). **P*<0.05 vs. SE. Data are expressed as mean ± SEM. Data were analyzed using Student's t-test.

Fig. S11

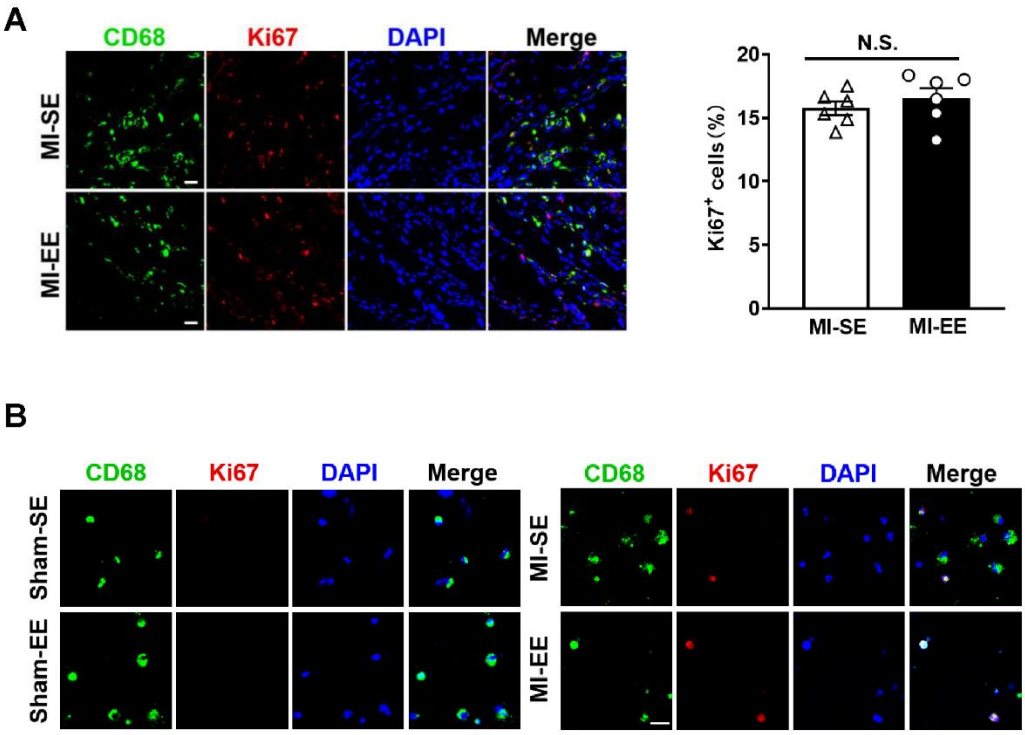

Fig. S11. Effects of EE on the proliferation of macrophages in infarcted hearts of mice. (A) Immunofluorescence staining for CD68 (green) and Ki67 (red) in the infarct areas of the SE and EE mice at 14 days after MI. Scale bars, 20μm. The percentage of $Ki67^+$ cells was expressed as $CD68^+$ $Ki67^+$cells/$CD68^+$cells (n=6). **(B)** Representative immunofluorescence staining for CD68 (green) and Ki67 (red) in $Ly6C^{low}$ macrophages isolated from the hearts of the SE and EE mice at 14 days after MI or sham surgery. Scale bars, 50 μm. Data are expressed as mean ± SEM. Data were analyzed using Student's t-test.

Fig. S12

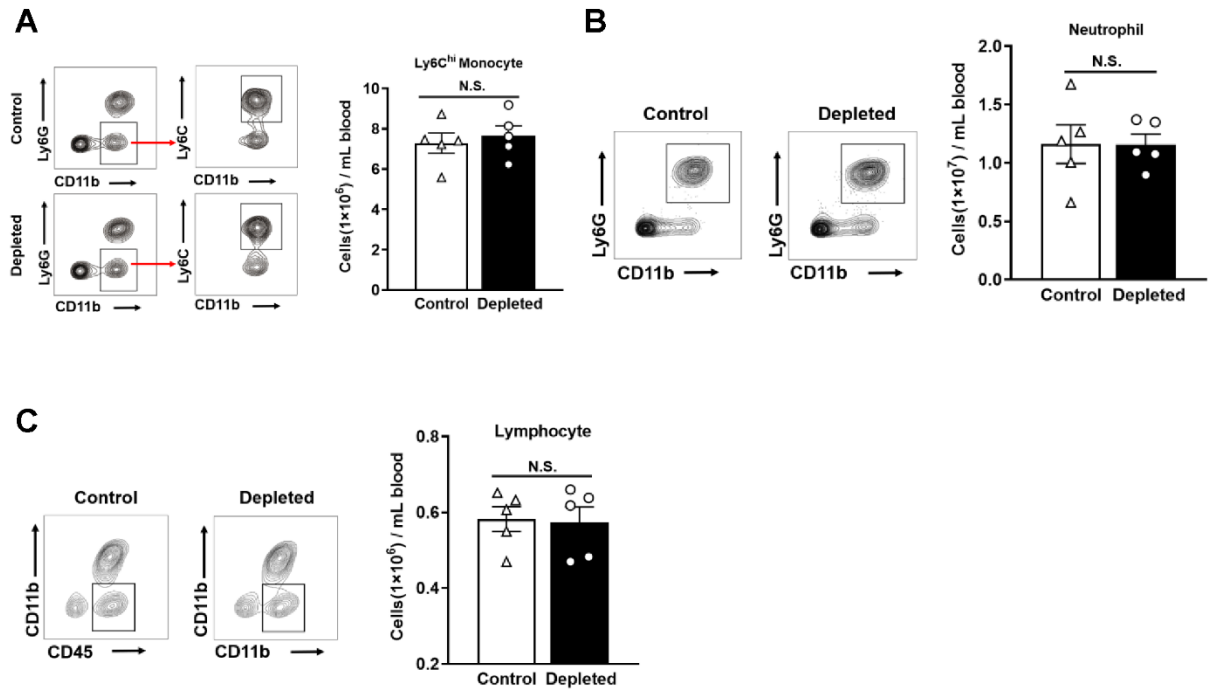

Fig. S12. The influence of cardiac resident macrophages depletion on other cell populations. **(A)** Gating strategy for $CD45^{+}CD11b^{+}Ly6G^{-}Ly6C^{high}$ monocytes in the peripheral blood obtained from $Cx3cr1^{CreER}\times R26^{Td/DTR}$ (depleted) and $Cx3cr1^{CreER}\times R26^{Td/+}$ (control) mice after DT injection. Flow cytometry-based quantification of $Ly6C^{high}$ monocytes (n=5). **(B)** Gating strategy for $CD45^{+}CD11b^{+}Ly6G^{hi}$ neutrophils in the peripheral blood of the depleted and control mice after DT injection. Flow cytometry-based quantification of neutrophils (n=5). **(C)** Gating strategy for $CD45^{+}CD11b^{-}$ lymphocytes in the peripheral blood of the depleted and control mice. Flow cytometry-based quantification of lymphocytes (n=5). Data are expressed as mean ± SEM. Data were analyzed using Student's t-test.

Fig. S13

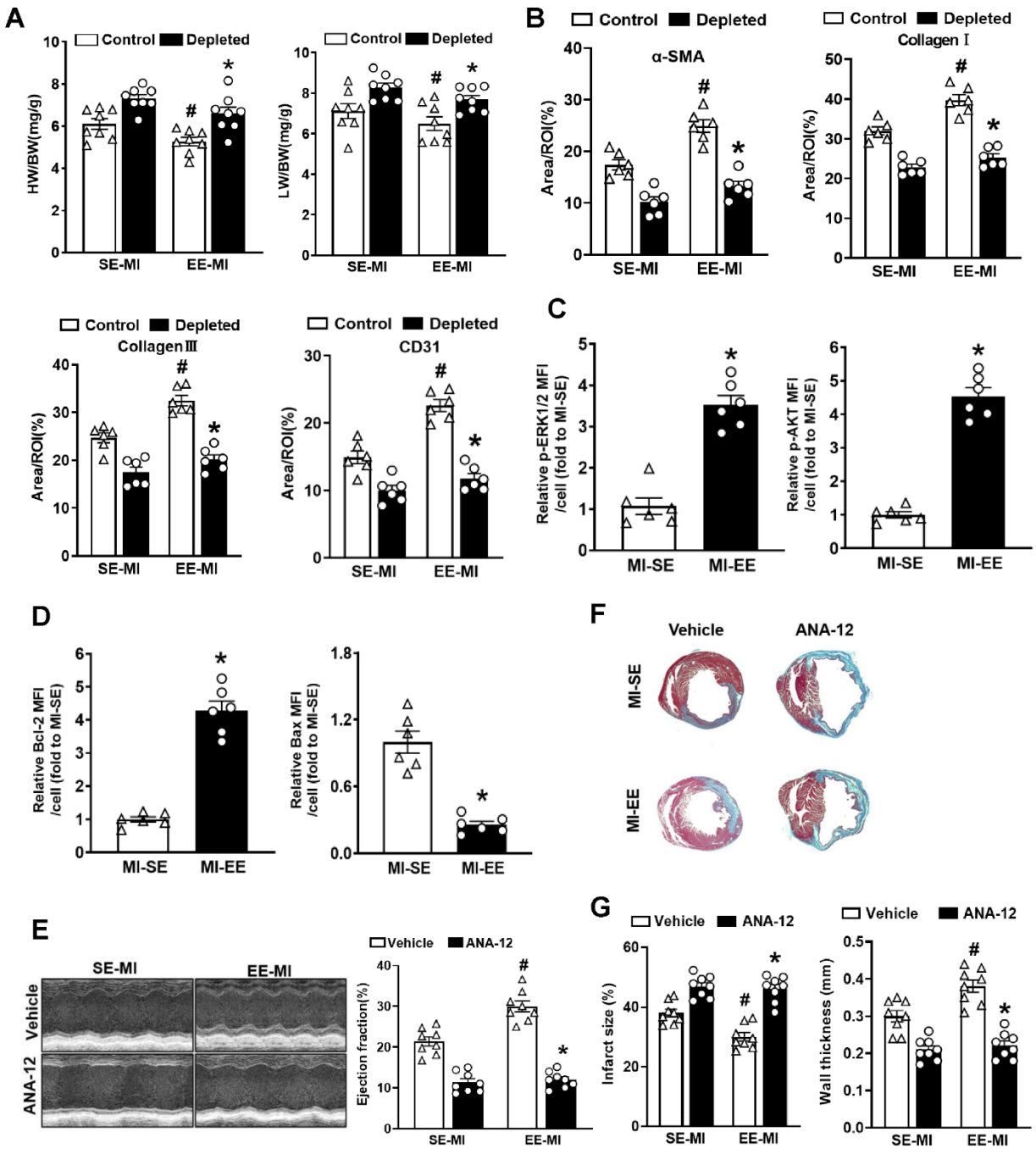
A
Control
Depleted
HW/BW(mg/g)
LW/BW(mg/g)
SE-MI
EE-MI
B
α-SMA
Collagen I
Collagen III
CD31
Area/ROI(%)
C
Relative p-ERK1/2 MFI /cell (fold to MI-SE)
Relative p-AKT MFI /cell (fold to MI-SE)
MI-SE
MI-EE
D
Relative Bcl-2 MFI /cell (fold to MI-SE)
Relative Bax MFI /cell (fold to MI-SE)
F
Vehicle
ANA-12
E
Ejection fraction(%)
G
Infarct size (%)
Wall thickness (mm)

Fig. S13. Effects of resident cardiac macrophages and the BDNF-TrkB signaling in EE-mediated cardio-protection. (A) Comparison of the HW/BW (mg/g) and LW/BW (mg/g) values between depleted mice and controls. HW, heart weight, LW, lung weight, BW, body weight (n=8-9). #P<0.05 vs. SE-MI. *P<0.05 vs. control. **(B)** Quantification of the percentage of α-SMA, collagen I, collagen III, and CD31 in the scar tissue (n=6). #P<0.05 vs. SE-MI. *P<0.05 vs. control. **(C)** Quantitation of p-ERK1/2 and p-AKT signaling in $CCR2^{-}MHCII^{low}$ macrophages sorted from infarcted hearts of SE and EE mice (n = 6). *P < 0.05 vs. MI-SE. **(D)** Quantitation of Bcl-2 and Bax signaling in $CCR2^{-}MHCII^{low}$ macrophages sorted from infarcted hearts of SE and EE mice (n = 6). *P < 0.05 vs. MI-SE. **(E)** Echocardiographic analysis of EF value of ANA-12 and vehicle mice at day 14 post MI after SE and EE housing (n = 8). #P < 0.05 vs. SE-MI. *P < 0.05 vs. vehicle. **(F-G)** Masson staining of cardiac tissue obtained from ANA-12 and vehicle mice at day 14 post MI after SE and EE housing. Quantitative analysis of infarct size and wall thickness (n = 8). # P < 0.05 vs. SE-MI. *P < 0.05 vs. vehicle. Data are expressed as mean ± SEM. Data were analyzed using two-way ANOVA followed by Bonferroni post hoc analysis.

Fig. S14

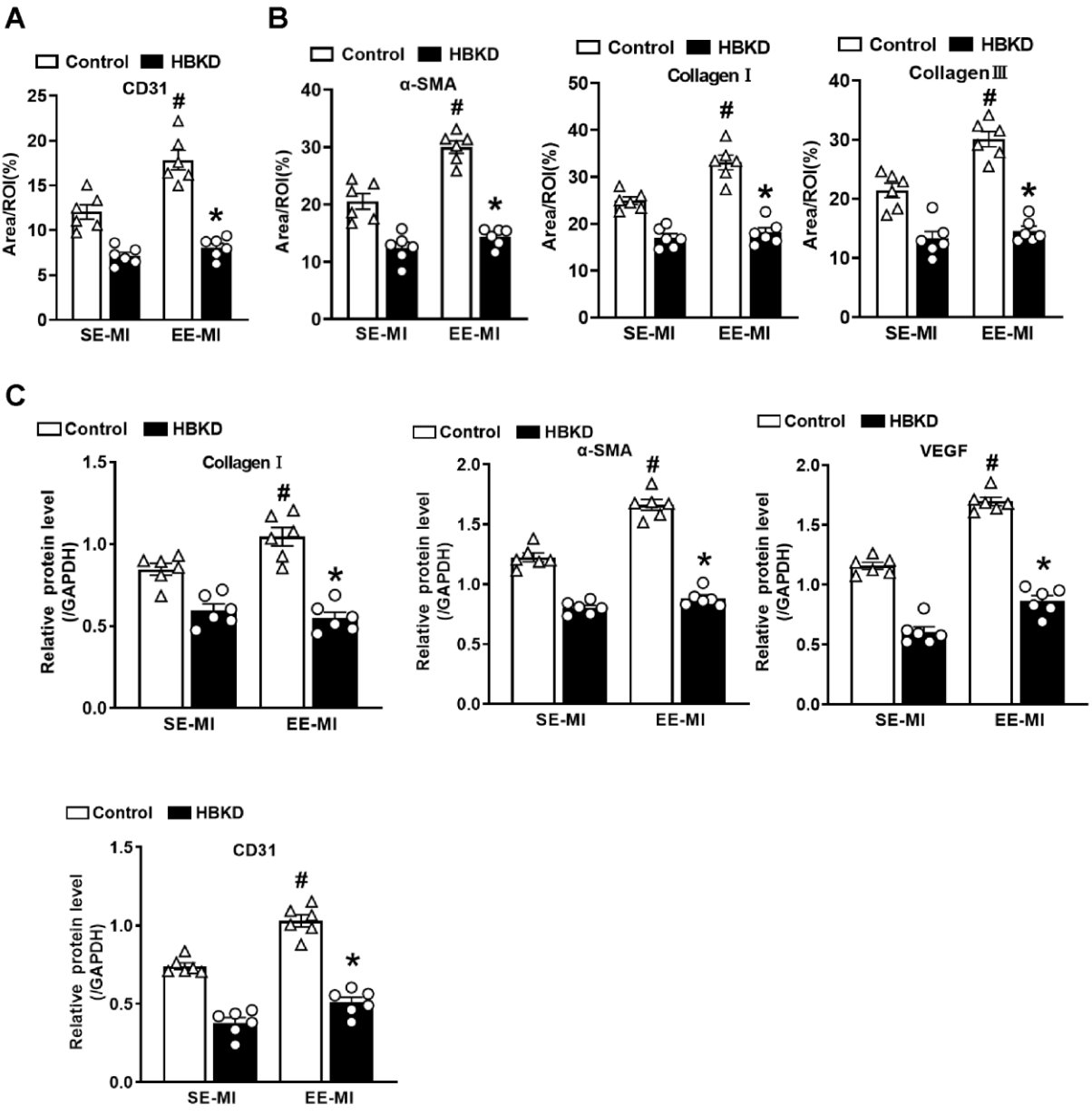
A
Control
HBKD
CD31
Area/ROI(%)
SE-MI
EE-MI
B
α-SMA
Collagen Ⅰ
Collagen Ⅲ
C
Relative protein level (/GAPDH)
VEGF

Fig. S14. Effects of hypothalamic BDNF knockdown on ECM and angiogenesis in infarcted tissues. (A) Quantification of the percentage of CD31 in Fig. 8F (n=6). # $P < 0.05$ vs. SE-MI. *$P < 0.05$ vs. Control. **(B)** Quantification of the percentage of α-SMA, collagen I, and collagen III in Fig. 8G (n=6). # $P < 0.05$ vs. SE-MI. *$P < 0.05$ vs. Control. **(C)** Quantification of collagen I, α-SMA, VEGF, and CD31 bands in Figure 8H were performed by densitometry and normalized to GAPDH (n=6). # $P < 0.05$ vs. SE-MI. *$P < 0.05$ vs. Control. Data are expressed as mean ± SEM. Data were analyzed using two-way ANOVA followed by Bonferroni post hoc analysis.

Fig. S15

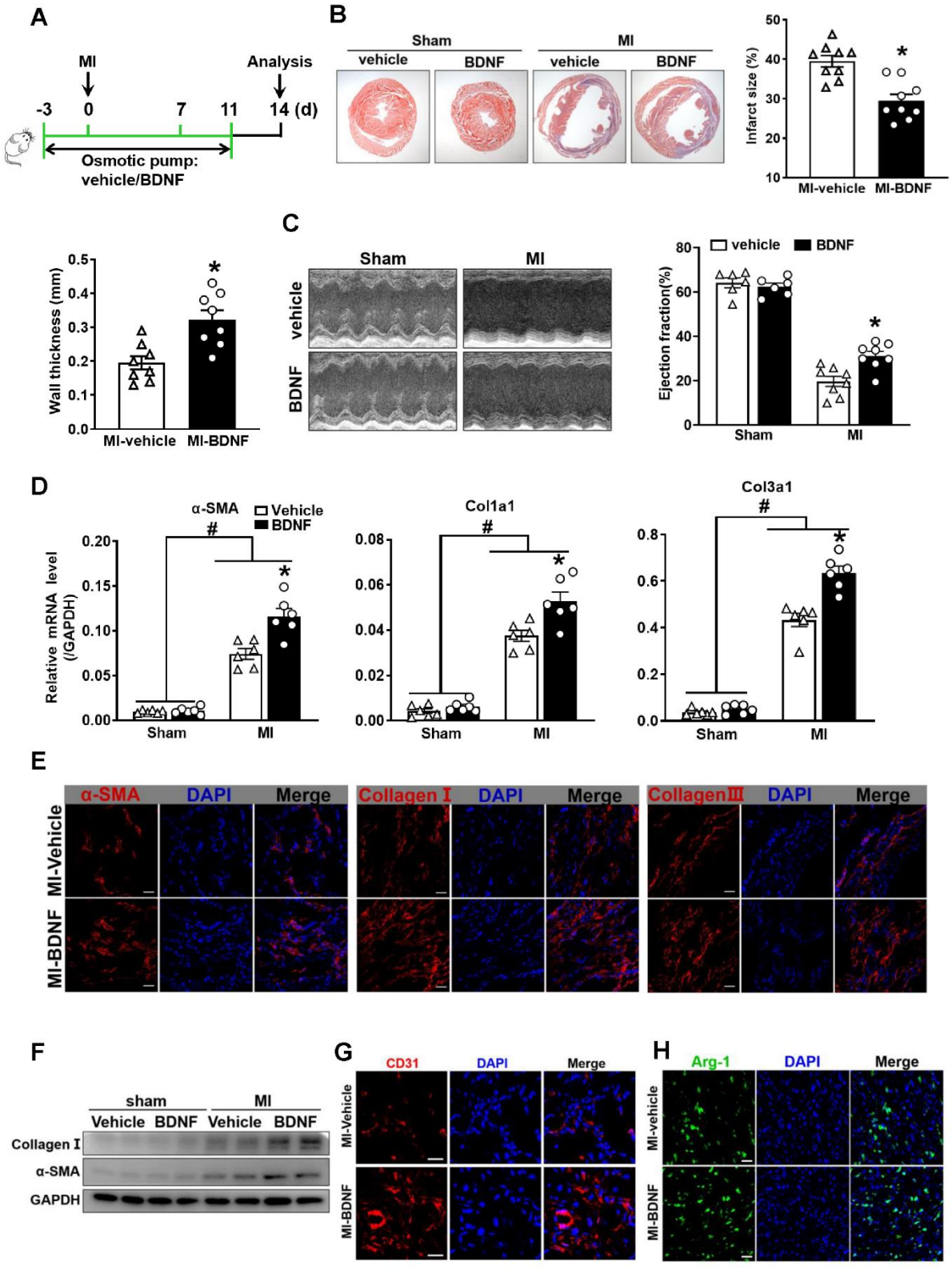
A
MI
Analysis
-3
0
7
11
14 (d)
Osmotic pump:
vehicle/BDNF
B
Sham
MI
vehicle
BDNF
vehicle
BDNF
Infarct size (%)
MI-vehicle
MI-BDNF
C
Wall thickness (mm)
MI-vehicle
MI-BDNF
Sham
MI
vehicle
BDNF
Ejection fraction(%)
vehicle
BDNF
Sham
MI
D
α-SMA
Vehicle
BDNF
Relative mRNA level (/GAPDH)
Col1a1
Col3a1
Sham
MI
E
α-SMA
DAPI
Merge
Collagen I
Collagen III
MI-Vehicle
MI-BDNF
F
sham
MI
Vehicle
BDNF
Vehicle
BDNF
Collagen I
α-SMA
GAPDH
G
CD31
DAPI
Merge
MI-Vehicle
MI-BDNF
H
Arg-1
DAPI
Merge
MI-vehicle
MI-BDNF

Fig. S15. Hypothalamic BDNF infusion mimics the cardioprotective effects of EE. (A) Timeline diagram of the experimental procedures. **(B)** Representative Masson staining of cardiac tissue obtained from vehicle- and BDNF-treated mice at day 14 after MI or sham operation. Quantitative analysis of infarct size and wall thickness (n = 8). *P < 0.05 vs. MI-vehicle. **(C)** Echocardiographic analysis of EF value at day 14 post- MI or sham operation (n = 6 for sham, n = 8 for MI). *P < 0.05 vs. MI-vehicle. **(D)** mRNA expression of α-SMA, Col1a1, and Col3a1 in scar tissue at day 14 post-MI or sham operation (n = 6). *P < 0.05 vs. MI-vehicle, #P < 0.05 vs. sham. **(E)** Immunostaining analyses of α-SMA, collagen I, and collagen III in infarct areas at 14 days after MI (Scale bars, 20 μm). **(F)** Western blot analyses of collagen I and α-SMA protein expression in the scar tissue at day 14 after MI or sham surgery. **(G)** Immunostaining of CD31 was performed on infarct sections collected at day 14 after MI (Scale bars, 50 μm). **(H)** Immunostaining of Arg-1 was performed on infarct sections collected at day 14 after MI (Scale bars, 50 μm). Data are expressed as mean ± SEM. Data in **(D)** were analyzed using two-way ANOVA followed by Bonferroni post hoc analysis. Data in **(B)** and **(C)** were analyzed using Student's t-test.

Fig. S16

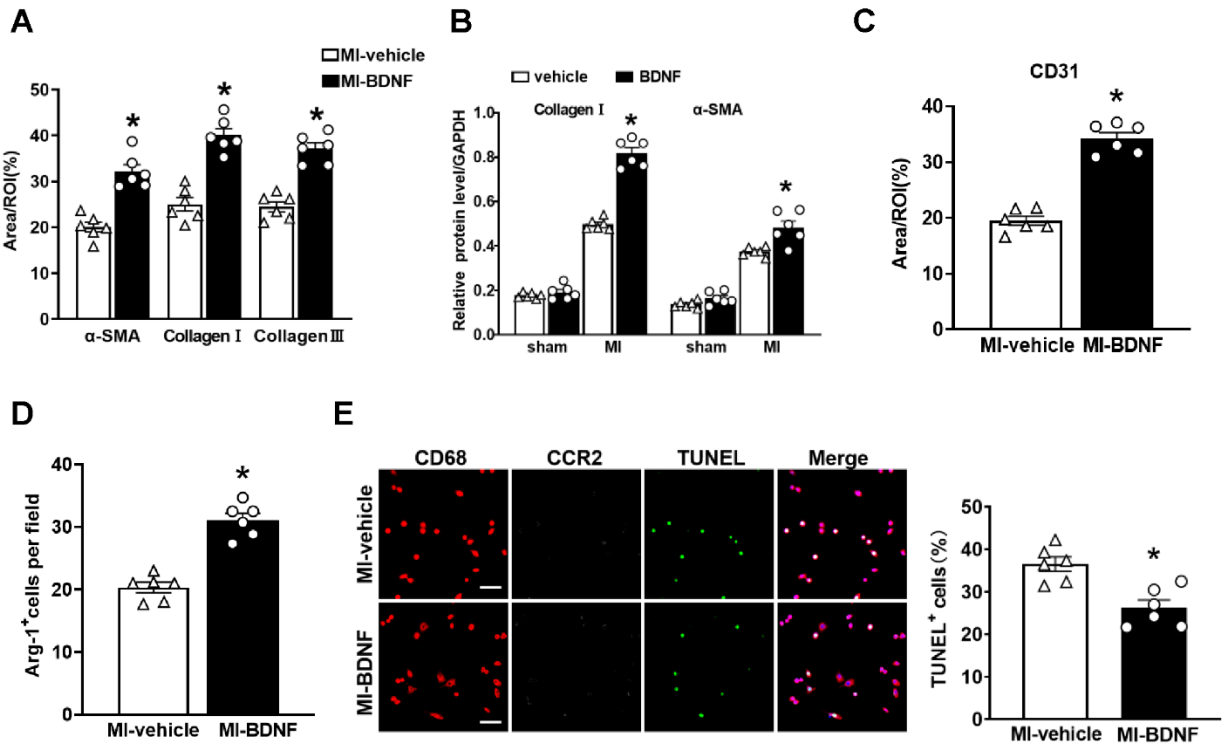

Fig. S16. Hypothalamic infusion of BDNF enhances EE-mediated cardiac repair. (A) Quantification of the percentage of α-SMA, collagen I, and collagen III in Fig. S15E (n=6). *P < 0.05 vs. MI-vehicle. **(B)** Quantification of collagen I and α-SMA bands in Fig. S15F (n=6). *P < 0.05 vs. Vehicle. **(C)** Quantification of $CD31^+$ areas in injured hearts as shown in Fig. S15G (n=6). P<0.05 vs. MI-vehicle. **(D)** Quantification of Arg-1^+ cells in each field as shown in Fig. S15H (n=6). P<0.05 vs. MI-vehicle. **(E)** Representative immunostaining for CD68 (red), CCR2 (white), and TUNEL (green) in $CCR2^-MHCII^{low}$ macrophages sorted from hearts at day 14 post- MI (Scale bars, 50 μm). Data are expressed as mean ± SEM. Data were analyzed using Student's t-test.

Table S1. Basic cardiac function parameters at day 14 post-MI.

Group	SE-Sham	EE-Sham	SE-MI	EE-MI
N	8	8	9	9
HW/BW (mg/g)	4.93±0.52	4.89±0.30	7.63±1.71	6.27±0.95*
LW/BW (mg/g)	5.60±0.42	5.25±0.17	8.77±1.34	7.24±1.39*
LVEDD (mm)	4.16± 0.16	4.10 ±0.25	5.92±0.82	5.38±0.66
LVESD (mm)	3.07 ±0.17	2.94± 0.25	5.46±0.56	4.84±0.66*
FS (%)	41.27±2.88	42.54±1.85	9.36±2.68	12.88±2.36*
LVEDV (ul)	62.23±7.09	60.99±8.06	129.50±9.62	111.10±9.06*
LVESV (ul)	25.21±4.94	24.20±6.19	91.81±10.36	70.50±8.91*
EF (%)	71.81±4.59	73.48±2.89	17.14±6.38	24.60±5.08*
HR (beats/min)	501.7±23.57	500.1±22.87	505.0±30.35	507.4±24.01

Data are expressed as *mean* ± SEM. *$P < 0.05$ *vs.* SE-MI.

SE, Standard Environment; EE, Enriched Environment; LVEDD, left ventricular end-diastolic dimension; LVESD, left ventricular end-systolic dimension; FS, fractional shortening; LVEDV, left ventricular end-diastolic volume; LVESV, left ventricular end-systolic volume; EF, ejection fraction; HR, heart rate.

Table S2. Primers for real-time PCR analysis in mice.

Gene	Sense	Anti-sense
BDNF	TCATACTTCGGTTGCATGAAGG	AGACCTCTCGAACCTGCCC
α-SMA	GTCCCAGACATCAGGGAGTAA	TCGGATACTTCAGCGTCAGGA
Collagen I	GCTCCTCTTAGGGGCCACT	CCACGTCTCACCATTGGGG
Collagen III	CTGTAACATGGAAACTGGGGAAA	CCATAGCTGAACTGAAAACCACC
IL-1β	AGCTCTCCACCTCAATGGAC	GACAGGCTTGTGCTCTGCTT
IL-6	TCCATCCAGTTGCCTTCTTG	GGTCTGTTGGGAGTGGTATC
TNF-α	ACGGCATGGATCTCAAAGAC	CGGACTCCGCAAAGTCTAAG
iNOS	GTTCTCAGCCCAACAATACAAGA	GTGGACGGGTCGATGTCAC
MMP-9	GCAGAGGCATACTTGTACCG	TGATGTTATGATGGTCCCACTTG
IL-10	AGCCTTATCGGAAATGATCCAGT	GGCCTTGTAGACACCTTGGT
TGF-β1	TGTTAAAACTGGCATCTGA	GTCTCTTAGGAAGTAGGT
VEGF	GCACATAGAGAGAATGAGCTT	CCCTCCGCTCTGAACAAGGCT
CD31	ACGCTGGTGCTCTATGCAAG	TCAGTTGCTGCCCATTCATCA
bFGF	CTGCTGGGGGTCTACCAAG	CTGCGCCTACCACTGTTCC
HGF	AGGTGACCTTTGCTTTCCCG	ACGTAAAGCCCCTGTTCCTG
Agrp	ATGCTGACTGCAATGTTGCTG	CAGACTTAGACCTGGGAACTCT
Lepr	TGGTCCCAGCAGCTATGGT	ACCCAGAGAAGTTAGCACTGT
Npy	ATGCTAGGTAACAAGCGAATGG	TGTCGCAGAGCGGAGTAGTAT
Ntrk2	CTGGGGCTTATGCCTGCTG	AGGCTCAGTACACCAAATCCTA
Sgk1	CTGCTCGAAGCACCCTTACC	TCCTGAGGATGGGACATTTTCA
Vgf	GTCAGACCCATAGCCTCCC	CTCGGACTGAAATCTCGAAGTTC
GAPDH	CCCTTATTGACCTCAACTACA	TGGTGAGGGGCCATCCACAGTCTTCTG

Legends for Movies

Movie S1: The video showed the state of mice living under SE condition.

Movie S2: The video showed the state of mice living under EE condition.